



Full communication

Bipolar anodic electrochemical exfoliation of graphite powders

Hideki Hashimoto^{a,*}, Yusuke Muramatsu^a, Yuta Nishina^{b,c,**}, Hidetaka Asoh^a^a Department of Applied Chemistry, School of Advanced Engineering, Kogakuin University, 2665-1 Nakano, Hachioji, Tokyo 192-0015, Japan^b Research Core for Interdisciplinary Sciences, Okayama University, 3-1-1 Tsushimanaka, Kita-ku, Okayama 700-8530, Japan^c Graduate School of Natural Science and Technology, Okayama University, 3-1-1 Tsushimanaka, Kita-ku, Okayama 700-8530, Japan

ARTICLE INFO

Keywords:

Graphite
Graphene
Graphene oxide
Electrochemical exfoliation
Anode
Bipolar electrochemistry

ABSTRACT

The electrochemical exfoliation of graphite has attracted considerable attention as a method for large-scale, rapid production of graphene and graphene oxide (GO). As exfoliation typically requires direct electrical contact, and is limited by the shape and/or size of the starting graphite, treatment of small graphite particles and powders, the typical form available commercially, is extremely difficult. In this study, GO nanosheets were successfully prepared from small graphite particles and powders by a bipolar electrochemical process. Graphite samples were placed between two platinum feeder electrodes, and a constant current was applied between the feeder electrodes using dilute sulfuric acid as the electrolyte. Optical microscopy, atomic force microscopy, X-ray diffractometry, Raman spectroscopy, and X-ray photoelectron spectroscopy were employed to examine the samples obtained after electrolysis. The results obtained from these analyses confirmed that anodic electrochemical exfoliation occurs in the graphite samples, and the exfoliated samples are basically highly crystalline GO nanosheets with a low degree of oxidation (C/O = 3.6–5.3). This simple electrochemical method is extremely useful for preparing large amounts of graphene and GO from small particles of graphite.

1. Introduction

Graphene, a two-dimensional sheet material comprising hexagonal close-packed carbon atoms bonded by sp^2 hybrid orbitals, exhibits superior electrical, optical, magnetic, mechanical, and chemical properties. For these reasons graphene has attracted considerable attention in physics, electronics, and materials science [1–3]. Although large pieces of low-defect graphene are typically prepared by chemical vapor deposition, large-scale production is difficult due to the need for expensive experimental equipment, high temperature conditions, and the long reaction time. Meanwhile, one of the most promising graphene analogues for practical applications is its oxidized form, graphene oxide (GO), due to its unique, tunable chemical properties originating from the presence of various functional groups on its surface [1–3]. GO can be prepared by the top-down chemical exfoliation of graphite. However, the preparation of GO typically requires large amounts of a strong acid and an oxidant, as well as having a long reaction time. Hence, it is important to develop a simple process for the large-scale production of GO.

The electrochemical exfoliation of graphite, induced by the electrochemical intercalation of ions into the graphite layers [4–12], is thought to be a feasible method for large-scale, rapid production.

Although cathodic exfoliation typically produces largely non-oxidized, low-defect graphene due to the reductive environment of the cathode, expensive and hazardous electrolytes (e.g., Li^+ /propylene carbonate, acetonitrile, and *N*-methyl-2-pyrrolidone) are required, as well as having a long reaction time. On the other hand, anodic exfoliation typically results in GO due to the oxidative environment of the anode. This has the advantage of using cost-effective electrolytes such as sulfuric acid [6,7] and also has an extremely short reaction time (< 1 h). In addition, the degree of oxidation can be reduced by using appropriate electrolyte additives [13–15]. Hence, the anodic exfoliation of graphite is an extremely attractive approach for the mass production of GO with a tunable degree of oxidation.

As direct electrical contact is typically needed for an electrochemical process, it is extremely difficult to treat small graphite particles, flakes, and powders, the forms in which it is typically available commercially. A no-contact electrochemical process that can easily treat these types of graphite would be promising as a breakthrough process. In the past decade, a wireless approach for electrode reactions referred to as bipolar electrochemistry has attracted considerable attention in materials science and dynamic systems [16–18]. A bipolar electrode is an electrically conductive material that is placed between two feeder electrodes in an electrolyte solution. On application of an

* Corresponding author.

** Correspondence to: Y. Nishina, Research Core for Interdisciplinary Sciences, Okayama University, 3-1-1 Tsushimanaka, Kita-ku, Okayama 700-8530, Japan.

E-mail addresses: hideki-h@cc.kogakuin.ac.jp (H. Hashimoto), nisina-y@cc.okayama-u.ac.jp (Y. Nishina).

external electric field to the two feeder electrodes, electrochemical reactions, i.e., oxidation and reduction, occur at the extremities (poles) of the bipolar electrode without any direct electrical connection. In this study, inspired by the concept of bipolar electrochemistry, the electrochemical anodic oxidation and exfoliation of a small particle of graphite and of graphite powder is carried out at a low voltage using industrially utilized sulfuric acid as the electrolyte.

2. Materials and methods

A graphite plate purchased from Alfa Aesar was used as the starting material. It was cut into a smaller plate (30 mm × 10 mm × 1 mm), a particle (1 mm × 1 mm × 1 mm), and powder (20–500 μm), which were subsequently used as bipolar electrodes. The bipolar electrodes were degreased with acetone before use. Two platinum plates (30 mm × 30 mm × 2 mm) were used as the feeder electrodes. The graphite plate was placed in a direction perpendicular to the feeder electrodes. The graphite particle or powder was put into an insulating mesh filter bag placed between the feeder electrodes. The distance between the two feeder electrodes was adjusted to 20 mm. A constant current of 2450 A m⁻² was applied using a direct current (DC) power supply (maximum voltage: 250 V) between the two feeder electrodes using 1–500 mmol dm⁻³ sulfuric acid as the electrolyte (volume: 0.5 dm³). The initial temperature of the electrolyte was adjusted to 10 °C, the electrolyte was stirred using a magnetic stirrer at 300 rpm during the process, and the electrolysis was carried out for 10–90 min. After the process was complete, the product was collected, and washed several times with deionized water and ethanol by vacuum filtration. The obtained samples were characterized by optical microscopy (BX51M, Olympus), X-ray diffractometry (Miniflex600, Rigaku), X-ray photoelectron spectroscopy (XPS, JSP9030, JEOL), Raman spectroscopy (T64000, Horiba Jobin Yvon Inc.), transmission electron microscopy (JEM-2100, JEOL), and atomic force microscopy (SPM-9700HT, Shimadzu). Detailed conditions for the XPS measurements and Raman spectroscopy are given in the Supplementary Information.

3. Results and discussion

Prior to the treatment of the powder samples, the graphite plate was tested to examine the effect of the electrolyte concentration on the electrochemical exfoliation of graphite. The distance between the two feeder electrodes was adjusted to 20 mm, the graphite plate was placed in a direction perpendicular to the feeder electrodes, and a constant current of 2450 A m⁻² was applied between the two feeder electrodes for 60 min using 1–500 mmol dm⁻³ sulfuric acid as the electrolyte. Fig. 1 shows the voltage–time (V–t) curves for the electrolysis. With an electrolyte concentration of 1 mmol dm⁻³, the voltage increased rapidly and reached the upper limit of the DC power supply (i.e., 250 V). However, at an electrolyte concentration > 10 mmol dm⁻³, the initial increase in the voltage gradually reduced and attained a steady value, and as the electrolyte concentration increased, the steady value of the voltage decreased. The temperature of the electrolyte initially increased and then attained a steady value after 10 min (Fig. S1 in the Supplementary Information). This temperature change could be related to the initial increase in the voltage. With an increase in the electrolyte concentration and a decrease in the steady voltage, the temperature increase was suppressed (Fig. S1).

The weights of the initial sample of graphite (w_i) and the exfoliated product (w_c) were measured, and the exfoliation ratio (w_c/w_i), a simple and rough indication of exfoliation progress, was calculated for each set of conditions. The exfoliation ratio and average voltage during electrolysis were plotted as a function of the electrolyte concentration (Fig. 2). Also shown in Fig. 2 (inset) are photographs of the bipolar electrode (the graphite plate) after electrolysis. The photographs revealed that exfoliation is initiated at the edge of the graphite plate facing the cathode of the feeder electrode, i.e., the anodic pole of the

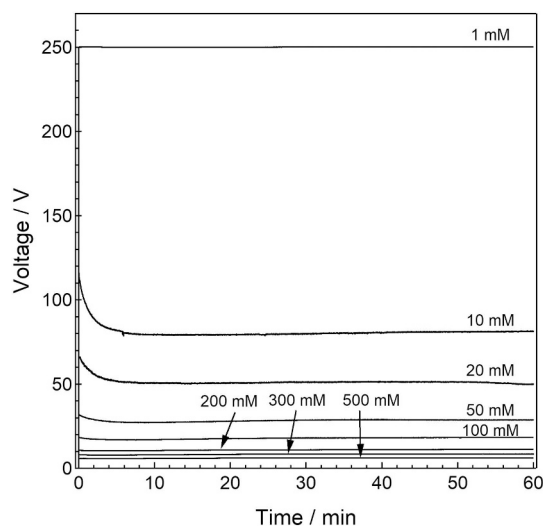


Fig. 1. V–t curves for the constant current electrolysis using various sulfuric acid concentrations. The current was applied between two Pt feeder electrodes, and a graphite plate was used as the bipolar electrode.

bipolar electrode, while no exfoliation was observed at the edge of the graphite plate facing the anode of the feeder electrode, i.e., the cathodic pole of the bipolar electrode where hydrogen gas generation occurs. The results show that exfoliation of the bipolar electrode occurs predominantly at the anodic site in this system. The amount of exfoliated graphite depends on the electrolyte concentration. With an increase in the electrolyte concentration, the exfoliation ratio increased, exhibiting a local maximum at an electrolyte concentration of 10–20 mmol dm⁻³, and then decreased at electrolyte concentrations > 50 mmol dm⁻³. Fig. 3a shows the optical microscopy image of the sample electrolyzed in the 20 mmol dm⁻³ electrolyte that generated a high exfoliation ratio. Several thin laminated flakes were observed, indicative of the delamination of the graphite layer without a direct electrical connection. Fig. 3b and c shows TEM images of the laminated flakes. The extremely thin sheets observed in the TEM images and the well-defined single crystalline electron-diffraction pattern (inset of Fig. 3b) demonstrated that they are crystalline graphene-like nanosheets. Figs. S2 and S3 in the Supplementary Information show further characterization results: The thin laminated flakes were GO nanosheets with a low degree of oxidation. Further details will be given later. From the viewpoint of the exfoliation ratio, the optimal electrolyte concentration was determined to be 10–20 mmol dm⁻³ in this experimental setup. Fig. S4 in the Supplementary Information plots the exfoliation ratio, which approximately indicates the degree of exfoliation, against the electrolysis time using 20 mmol dm⁻³ sulfuric acid. The exfoliation ratio was proportional to the electrolysis time, and the graphite plate completely disappeared after 90 min. The exfoliated samples, comprising GO laminated flakes, were analogous to the sample shown in Fig. 3.

The same treatment using 20 mmol dm⁻³ sulfuric acid as the electrolyte was applied to a graphite particle (1 mm × 1 mm × 1 mm) and graphite powder (20–500 μm). To locate the samples between the two feeder electrodes, each sample was placed in an insulating mesh filter bag. Fig. 4a shows the photographs and V–t curves. The V–t curves for both the particle and the powder showed similar behavior. The voltage rapidly increased, gradually decreased, and then maintained a steady value of ~60 V. After electrolysis for 30 min, the filter bag turned black due to the dispersion of exfoliated material in the filter bag for both the particle and the powder. After electrolysis for 30 min, the 1-mm square particle had completely disappeared, indicating that exfoliation proceeds efficiently for 30 min. Fig. 4b shows the optical microscopy images of the powder sample before and after electrolysis. Although the powder comprises particles with diameters of 20–500 μm (Fig. 4b, left),

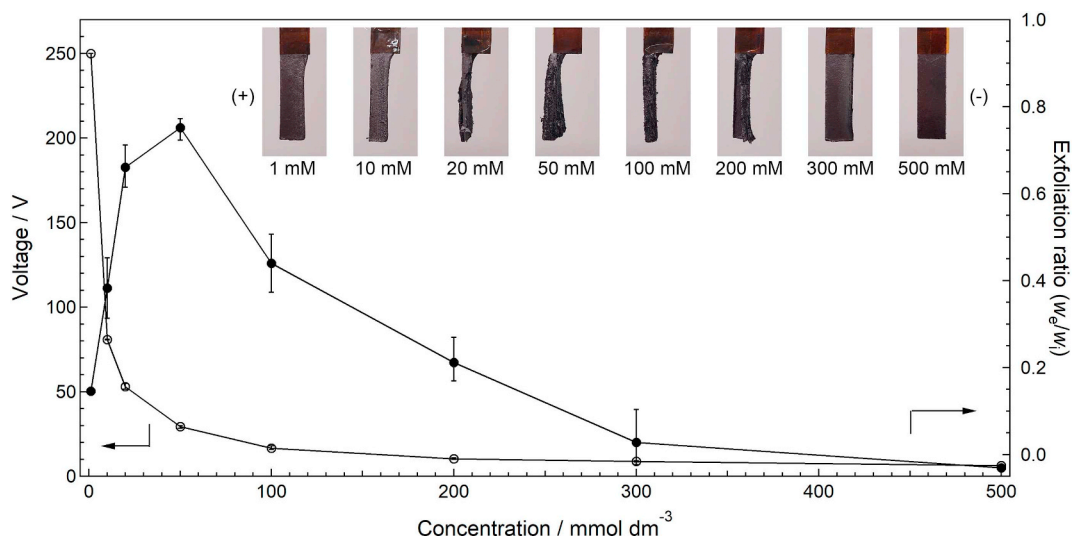


Fig. 2. Relationship between the exfoliation ratio and sulfuric acid concentration. In addition, the average voltage for each electrolysis shown in Fig. 1 was plotted. Electrolysis was carried out for 60 min, and the photographs of the graphite plates after electrolysis are shown. (+) and (-) represent the poles of the feeder electrodes.

the particles disappeared, and GO laminated flakes were observed after electrolysis for 30 min (Fig. 4b, right). Fig. 4c shows the AFM images of exfoliated GO. Although most of the flakes were 3–5-nm thick, thinner flakes (thickness < 2 nm) were also observed, possibly corresponding to partial mono- or bi-layers of the GO sheet.

The theoretical potential difference between the anode and cathode of bipolar electrodes [16,17] with a size of 1 mm or 20–500 μm was calculated to be 2.5 V or 0.05–1.25 V, respectively, for this experimental setup (distance between the feeder electrodes: 20 mm; applied steady voltage between feeder electrodes: ~ 60 V). This predicted voltage is less than the previously reported values at which the electrochemical exfoliation of graphite occurs using sulfuric acid electrolyte (3–10 V) [6,7]. Nevertheless, the electrochemical exfoliation of a small graphite particle and powder occurred in this experiment. This phenomenon has not been clarified thus far; however, the following factors could have a strong influence: (i) the water splitting reaction and active ion migration occurring in the electrolyte; (ii) the electrophoretic force received by graphite; (iii) the aggregation state of the graphite; and (iv) changes in the electrical properties of graphite and exfoliated products during electrolysis. Preliminarily, we have confirmed that a single graphite particle smaller than 500 μm could not be exfoliated under these conditions. Hence, the above possibilities option number (iii) would have a great influence on the bipolar anodic electrochemical

exfoliation of the powder. Note that the above discussion is only a tentative explanation. Clarification of the detailed mechanism should be an important future study.

Fig. S2 in the Supplementary information shows the XRD patterns of the graphite before electrolysis and the exfoliated samples produced using the plate, particle, and powder. The intensity of the main XRD peak corresponding to the graphite (002) plane drastically decreased for all exfoliated samples, indicating that the intercalation of sulfate ions and subsequent delamination occur successfully, regardless of the shape and size of the sample. However, the XRD peak intensity for the exfoliated product from the graphite plate was greater than those for the particle and powder. This is possibly related to differences in the way the samples were fixed between the two feeder electrodes. The plate was simply hung by a clip, and the exfoliated sample was freely suspended in the electrolyte. On the other hand, the particle and powder were contained in the filter bag, together with the exfoliated material. Hence, the exfoliated sample is additionally electrolyzed in the filter bag, promoting additional exfoliation. Further characterization by Raman spectroscopy and XPS (Fig. S3 in the Supplementary Information) is basically consistent with the XRD results, indicating that the exfoliated samples exhibit a disordered structure and oxygen species (C/O = 3.61–5.25). Hence, all exfoliated samples, whether from graphite plate, particle or powder, are shown to be GO nanosheets.

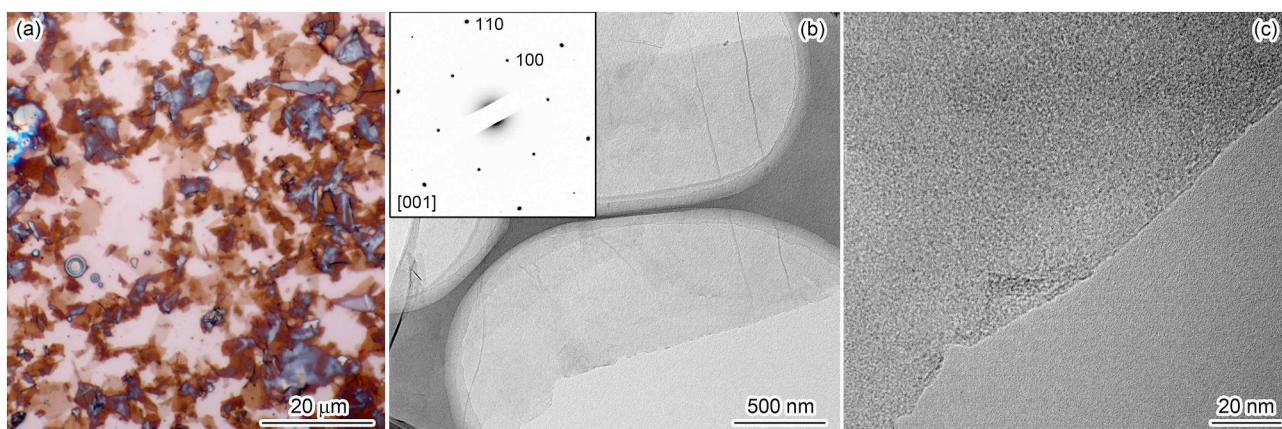


Fig. 3. (a) Optical microscopy image (b) low and (c) high magnification TEM images of the sample exfoliated using 20 mmol dm⁻³ sulfuric acid electrolyte. The inset image of (b) is the electron diffraction pattern of the corresponding TEM image for an incident beam irradiation from the [001] zone axis.

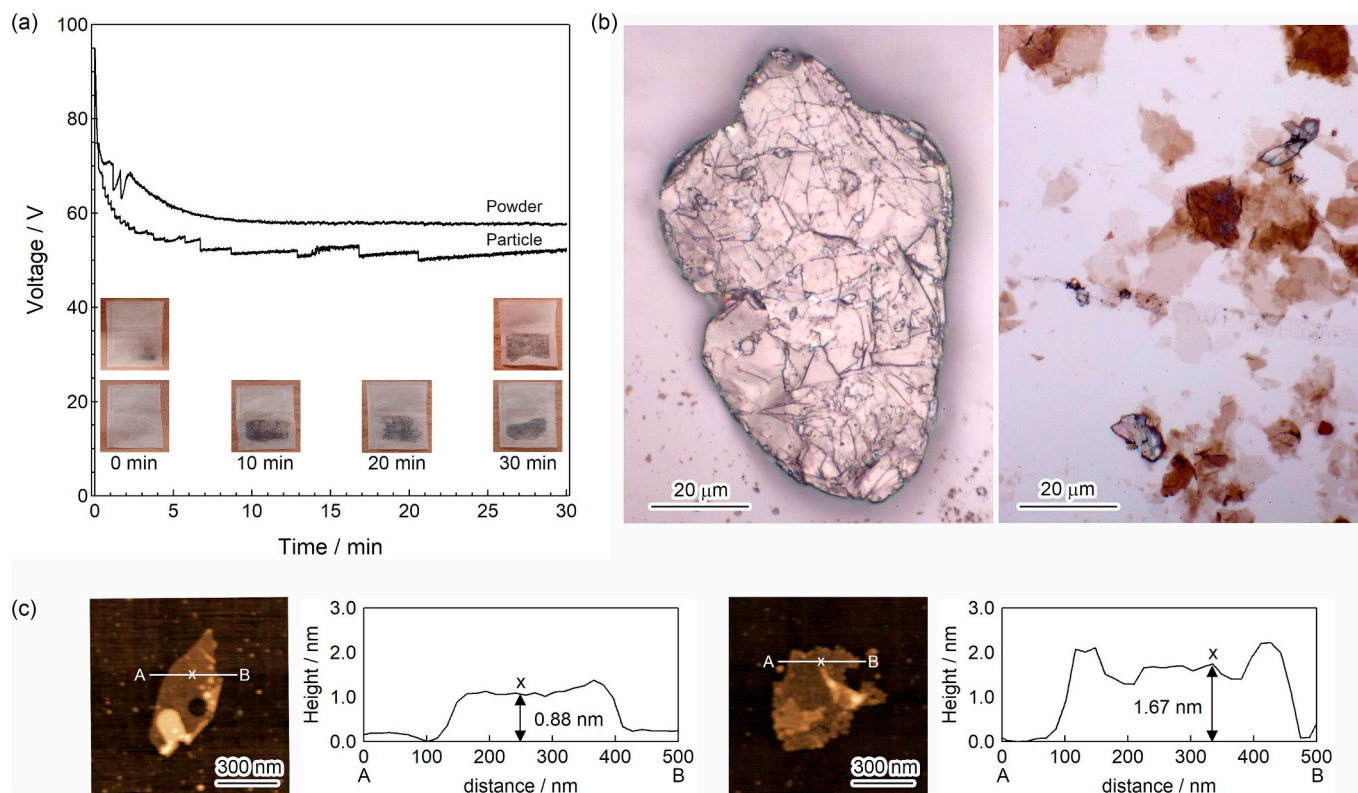


Fig. 4. (a) V–t curves for the constant current electrolysis using the 20 mmol dm⁻³ sulfuric acid electrolyte. A graphite particle and graphite powder contained in an insulating mesh filter bag were used as the bipolar electrodes. Photographs before and after electrolysis are also shown. (b) Optical microscopy images of the graphite powder before (left) and after (right) electrolysis. (c) AFM images and line scan profiles of the graphite powder after electrolysis.

The bipolar electrolysis of graphite powder has been reported previously [19]. This involved the cathodic electrochemical intercalation of tetrabutylammonium ions and subsequent mechanical high-shear exfoliation. Notably, exfoliation required an extremely high voltage of 1100 V, an organic electrolyte, and a specially designed experimental setup equipped with a grounded cage comprising an interlock system for safety. Furthermore, post treatment of the high-shear exfoliation products was required. The anodic process developed here produces exfoliated products using an extremely low voltage (~60 V), which is 20 times lower than that reported previously. Hence, this bipolar anodic electrochemical exfoliation approach can be viewed as a breakthrough process that could be adopted for the industrial mass production of graphene and GO.

4. Conclusions

A bipolar electrochemical exfoliation method was developed to exfoliate graphite in the form of small particles and powders. The electrolysis conditions were first optimized using a graphite plate, and then the process was applied to smaller graphite samples. The graphite samples were placed between two Pt feeder electrodes, and a constant current was applied using sulfuric acid as the electrolyte. Results obtained from optical microscopy, XRD, Raman spectroscopy, and TEM measurements revealed that GO nanosheets can be prepared from graphite regardless of its size and shape. Our method produced exfoliated graphite products using a voltage 20 times lower than the values reported previously for bipolar electrolysis processes, demonstrating immense potential for the large-scale production of graphene materials.

Acknowledgments

We thank Ms. Tomoko Ohkubo, Ms. Ikuyo Sugimoto, Mr. Campeon Benoit, and Mr. Dan Kawabe for helpful discussion and AFM, XPS, Raman, and TEM measurements. This study was financially supported by a Grant-in Aid for Challenging Exploratory Research [grant number 17K18994] from the Japan Society for the Promotion of Science and JST CREST [grant number JPMJCR18R3].

Appendix A. Supplementary data

Supplementary data to this article can be found online. Structure analysis of GO prepared by modified Hummers' method was reported previously [20,21]. Supplementary data to this article can be found online at <https://doi.org/10.1016/j.elecom.2019.06.001>.

References

- [1] Y. Zhu, S. Murali, W. Cai, X. Li, J.W. Suk, J.R. Potts, R.S. Ruoff, Graphene and graphene oxide: synthesis, properties, and applications, *Adv. Mater.* 22 (2010) 3906–3924.
- [2] X. Huang, Z. Yin, S. Wu, X. Qi, Q. He, Q. Zhang, Q. Yan, F. Boey, H. Zhang, Graphene-based materials: synthesis, characterization, properties, and applications, *Small* 7 (2011) 1876–1902.
- [3] A.C. Ferrari, F. Bonaccorso, V. Fal'ko, K.S. Novoselov, S. Roche, P. Boggild, S. Borini, F.H. Koppens, V. Palermo, N. Pugno, J.A. Garrido, R. Sordan, A. Bianco, L. Ballerini, M. Prato, E. Lidorikis, J. Kivioja, C. Marinelli, T. Ryhanen, A. Morigo, J.N. Coleman, V. Nicolosi, L. Colombo, A. Fert, M. Garcia-Hernandez, A. Bachtold, G.F. Schneider, F. Guinea, C. Dekker, M. Barbone, Z. Sun, C. Galiotis, A.N. Grigorenko, G. Konstantatos, A. Kis, M. Katsnelson, L. Vandersypen, A. Loiseau, V. Morandi, D. Neumaier, E. Treossi, V. Pellegrini, M. Polini, A. Tredicucci, G.M. Williams, B.H. Hong, J.H. Ahn, J.M. Kim, H. Zirath, B.J. van Wees, H. van der Zant, L. Occhipinti, A. Di Matteo, I.A. Kinloch, T. Seyller, E. Quesnel, X. Feng, K. Teo, N. Rupasinghe, P. Hakonen, S.R. Neil, Q. Tannock, T. Lofwander, J. Kinaret, Science and technology roadmap for graphene, related two-dimensional crystals, and hybrid systems, *Nanoscale* 7 (2015) 4598–4810.

- [4] N. Liu, F. Luo, H. Wu, Y. Liu, C. Zhang, J. Chen, One-step ionic-liquid-assisted electrochemical synthesis of ionic-liquid-functionalized graphene sheets directly from graphite, *Adv. Funct. Mater.* 18 (2008) 1518–1525.
- [5] G. Wang, B. Wang, J. Park, Y. Wang, B. Sun, J. Yao, Highly efficient and large-scale synthesis of graphene by electrolytic exfoliation, *Carbon* 47 (2009) 3242–3246.
- [6] C.Y. Su, A.Y. Lu, Y. Xu, F.R. Chen, A.N. Khlobystov, L.J. Li, High-quality thin graphene films from fast electrochemical exfoliation, *ACS Nano* 5 (2011) 2332–2339.
- [7] K. Parvez, R. Li, S.R. Puniredd, Y. Hernandez, F. Hinkel, S. Wang, X. Feng, K. Mullen, Electrochemically exfoliated graphene as solution-processable, highly conductive electrodes for organic electronics, *ACS Nano* 7 (2013) 3598–3606.
- [8] C.T.J. Low, F.C. Walsh, M.H. Chakrabarti, M.A. Hashim, M.A. Hussain, Electrochemical approaches to the production of graphene flakes and their potential applications, *Carbon* 54 (2013) 1–21.
- [9] H.J. Salavagione, Promising alternative routes for graphene production and functionalization, *J. Mater. Chem. A* 2 (2014) 7138–7146.
- [10] A.M. Abdelkader, A.J. Cooper, R.A. Dryfe, I.A. Kinloch, How to get between the sheets: a review of recent works on the electrochemical exfoliation of graphene materials from bulk graphite, *Nanoscale* 7 (2015) 6944–6956.
- [11] S. Yang, M.R. Lohe, K. Mullen, X. Feng, New-generation graphene from electrochemical approaches: production and applications, *Adv. Mater.* 28 (2016) 6213–6221.
- [12] J.I. Paredes, J.M. Munuera, Recent advances and energy-related applications of high quality/chemically doped graphenes obtained by electrochemical exfoliation methods, *J. Mater. Chem. A* 5 (2017) 7228–7242.
- [13] K.S. Rao, J. Sentilnathan, H.W. Cho, J.J. Wu, M. Yoshimura, Soft processing of graphene nanosheets by glycine-bisulfate ionic-complex-assisted electrochemical exfoliation of graphite for reduction catalysis, *Adv. Funct. Mater.* 25 (2015) 298–305.
- [14] C.H. Chen, S.W. Yang, M.C. Chuang, W.Y. Woon, C.Y. Su, Towards the continuous production of high crystallinity graphene via electrochemical exfoliation with molecular in situ encapsulation, *Nanoscale* 7 (2015) 15362–15373.
- [15] S. Yang, S. Brüller, Z.S. Wu, Z. Liu, K. Parvez, R. Dong, F. Richard, P. Samori, X. Feng, K. Mullen, Organic radical-assisted electrochemical exfoliation for the scalable production of high-quality graphene, *J. Am. Chem. Soc.* 137 (2015) 13927–13932.
- [16] S.E. Fosdick, K.N. Knust, K. Scida, R.M. Crooks, Bipolar electrochemistry, *Angew. Chem. Int. Ed.* 52 (2013) 10438–10456.
- [17] G. Loget, D. Zigah, L. Bouffier, N. Sojic, A. Kuhn, Bipolar electrochemistry: from materials science to motion and beyond, *Acc. Chem. Res.* 46 (2013) 2513–2523.
- [18] L. Koefoed, S.U. Pedersen, K. Daasbjerg, Bipolar electrochemistry—a wireless approach for electrode reactions, *Curr. Opin. Electrochem.* 2 (2017) 13–17.
- [19] E.T. Bjerglund, M.E.P. Kristensen, S. Stambula, G.A. Botton, S.U. Pedersen, K. Daasbjerg, Efficient graphene production by combined bipolar electrochemical intercalation and high-shear exfoliation, *ACS Omega* 2 (2017) 6492–6499.
- [20] N. Morimoto, T. Kubo, Y. Nishina, Tailoring the oxygen content of graphite and reduced graphene oxide for specific applications, *Sci. Rep.* 6 (2016) 21715.
- [21] N. Morimoto, H. Suzuki, Y. Takeuchi, S. Kawaguchi, M. Kunisu, C.W. Bielawski, Y. Nishina, Real-time, in situ monitoring of the oxidation of graphite: lessons learned, *Chem. Mater.* 29 (2017) 2150–2156.